

# Serum deprivation response inhibits breast cancer progression by blocking transforming growth factor- $\beta$ signaling

Yao Tian,<sup>1,2,3,5</sup> Yue Yu,<sup>1,2,3,5</sup> Li-Kun Hou,<sup>1,2,3</sup> Jiang-Rui Chi,<sup>1,2,3</sup> Jie-Fei Mao,<sup>1,2,3</sup> Li Xia,<sup>1,2,3</sup> Xin Wang,<sup>1,2,3</sup> Ping Wang<sup>2,4</sup> and Xu-Chen Cao<sup>1,2,3</sup>

<sup>1</sup>The First Department of Breast Cancer, Tianjin Medical University Cancer Institute and Hospital, National Clinical Research Center for Cancer, Tianjin; <sup>2</sup>Key Laboratory of Cancer Prevention and Therapy, Tianjin; <sup>3</sup>Key Laboratory of Breast Cancer Prevention and Therapy, Tianjin Medical University, Ministry of Education, Tianjin; <sup>4</sup>Department of Radiobiology, Tianjin Medical University Cancer Institute and Hospital, National Clinical Research Center for Cancer, Tianjin, China

## Key words

Breast cancer, epithelial–mesenchymal transition, progression, serum deprivation response, transforming growth factor- $\beta$

## Correspondence

Xu-Chen Cao, the First Department of Breast Cancer, Tianjin Medical University Cancer Institute and Hospital, Huanhuxi Road, Hexi District, Tianjin 300060, China.  
Tel: 86-022-23340123 ext. 2084; Fax: 86-022-23537796  
E-mail: caoxuchen@tmu.edu.cn  
and

Ping Wang, Department of Radiobiology, Tianjin Medical University Cancer Institute and Hospital, Huanhuxi Road, Hexi District, Tianjin 300060, China.  
Tel: 86-022-23537796; Fax: 86-022-23537796  
E-mail: wangping@tjmuch.com

## Funding Information

National Natural Science Foundation of China (Nos 81372843, 81472472 and 81502518), the National Science and Technology Support Program (No. 2015BAI12B15).

<sup>5</sup>These authors contributed equally to this work.

Received September 14, 2015; Revised December 28, 2015; Accepted January 2, 2016

*Cancer Sci* 107 (2016) 274–280

doi: 10.1111/cas.12879

**B**reast cancer is one of the most common malignancies in women worldwide and the second leading cause of cancer-related diseases in women, especially middle and old aged women, the incidence rate of which is still very high.<sup>(1,2)</sup> Although improvements in early detection and treatment have decreased breast cancer mortality rates in recent years, prevention and therapy of breast cancer remain a major public health concern. Unfortunately, the incomplete understanding of its carcinogenic mechanisms leads to difficulties in selecting targeted treatment and contributes to a low survival rate for patients with breast cancer.

Serum deprivation response factor (SDPR), also known as Cavin-2, is located on chr 2, q32-33, with the function of coding purified phospholipids binding protein of platelets. SDPR has been considered as a key substrate for protein kinase C (PKC) phosphorylation and this interaction determi-

nes the compartmentalization of PKC to caveolae.<sup>(3,4)</sup> SDPR was further confirmed to function in inducing membrane curvature and participate in the caveolae formation.<sup>(5,6)</sup> Caveolae is calcium channel related to gut electrophysiological pacing function and impacts the cell proliferation and migration.<sup>(7)</sup> Previous studies indicated that SDPR was significantly reduced in tumors of breast, kidney and prostate.<sup>(8–10)</sup> Recently, it has been demonstrated that downregulation of miR-206 induces the deformation of caveolae and suppresses cell proliferation and migration by upregulating SDPR expression.<sup>(11)</sup> These studies suggest that SDPR is a potential tumor suppressor. However, the mechanism of SDPR in breast cancer development and progression is still not clear.

In the present study, we investigated the function of SDPR in breast cancer progression. We found that the downregulation

© 2016 The Authors. Cancer Science published by John Wiley & Sons Australia, Ltd on behalf of Japanese Cancer Association.

This is an open access article under the terms of the Creative Commons Attribution-NonCommercial-NoDerivs License, which permits use and distribution in any medium, provided the original work is properly cited, the use is non-commercial and no modifications or adaptations are made.

of SDPR expression promotes breast cancer progression by induction of EMT through activation of TGF- $\beta$  signaling.

## Materials and Methods

**Reagents and antibodies.** Recombinant human TGF- $\beta$ 1 was purchased from R&D System. TGF- $\beta$  inhibitor SB-431542 was purchased from Selleck (Shanghai, China). The antibodies for SDPR (ab103230) and N-cadherin (ab18203) were purchased from Abcam (Cambridge, MA, USA). The antibodies for pSmad2/3 (9510), Smad2/3 (total; 8685), Cyclin D1 (2926), p21 (2946) and  $\beta$ -catenin (8480) were purchased from Cell Signaling (Beverly, MA, USA). The antibodies for Vimentin (sc-373717), E-cadherin (sc-7870) and  $\beta$ -actin (sc-47778) were purchased from Santa Cruz (Santa Cruz, CA, USA).

**Cell culture and tissue specimens.** MDA-MB-231, MCF7, T47D, MDA-MB-468, SKBR3 and MCF10A cell lines were obtained from the Type Culture Collection of the Chinese Academy of Sciences. MDA-MB-231 and SKBR3 cell lines were cultured in RPMI-1640 medium (Gibco, Grand Island, NY, USA) with 10% FBS (Gibco). MCF7, T47D and MDA-MB-468 cell lines were cultured in DMEM medium (Gibco) with 10% FBS. While MCF10A cell lines were supplemented with DMEM (Gibco) with 5% horse serum (Life Technologies, Grand Island, NY, USA), 10  $\mu$ g/mL insulin (Sigma, St Louis, MO, USA), 0.5  $\mu$ g/mL hydrocortisone (Sigma), 20 ng/mL EGF (R&D Systems, Redmond, WA, USA) and 100 ng/mL cholera toxin (Sigma). All the cells were supplemented with 1% penicillin/streptomycin (Gibco), in a 5% CO<sub>2</sub> and humidified atmosphere at 37°C.

Cancer specimens were obtained from Tianjin Medical University Cancer Institute and Hospital. Thirty cases of primary breast cancer tissue and the paired adjacent normal breast tissue specimens were included in the present study. After mastectomy surgery, the primary cancer tissues and the adjacent normal tissues were flash-frozen in liquid nitrogen and stored at -80°C. This study was approved by the Institutional Review Board of the Tianjin Medical University Cancer Institute and Hospital and written consent was obtained from all participants.

**RNA extraction and reverse transcription quantitative PCR.** The total RNA of cultured cells and surgically resected fresh breast tissues were extracted using mirVana PARIS kit (Life Technologies) according to the manufacturer's instructions. Reverse transcription was performed using a First Strand cDNA Synthesis kit (TakaRa, Dalian, China), according to the manufacturer's instructions. The real-time quantitative PCR was performed using GoTaq qPCR Master Mix (Promega, Madison, WI, USA) on a Bio-Rad iQ5 Optical System (Bio-Rad, Berkeley, CA, USA).  $\beta$ -actin was used as an internal control. The primers are listed in the Supplementary material.

**siRNA, transfection and generation of stable cell line.** siRNA targeting SDPR were bought from Guangzhou RiboBio. The targeting sequences of siRNA are listed in the supplementary material. For transfection, cells were plated at a density of  $2 \times 10^5$  cells/well in six-well plates. When the cells were 60% confluent, 50 nmol/L siRNA or 4  $\mu$ g SDPR-HA was transfected into cells using Lipofectamine 3000 (Invitrogen) according to the manufacturer's recommendations. After transfection, the RNA and protein were extracted after 24 and 48 h, respectively. SDPR cDNA was generated from MDA-MB-231

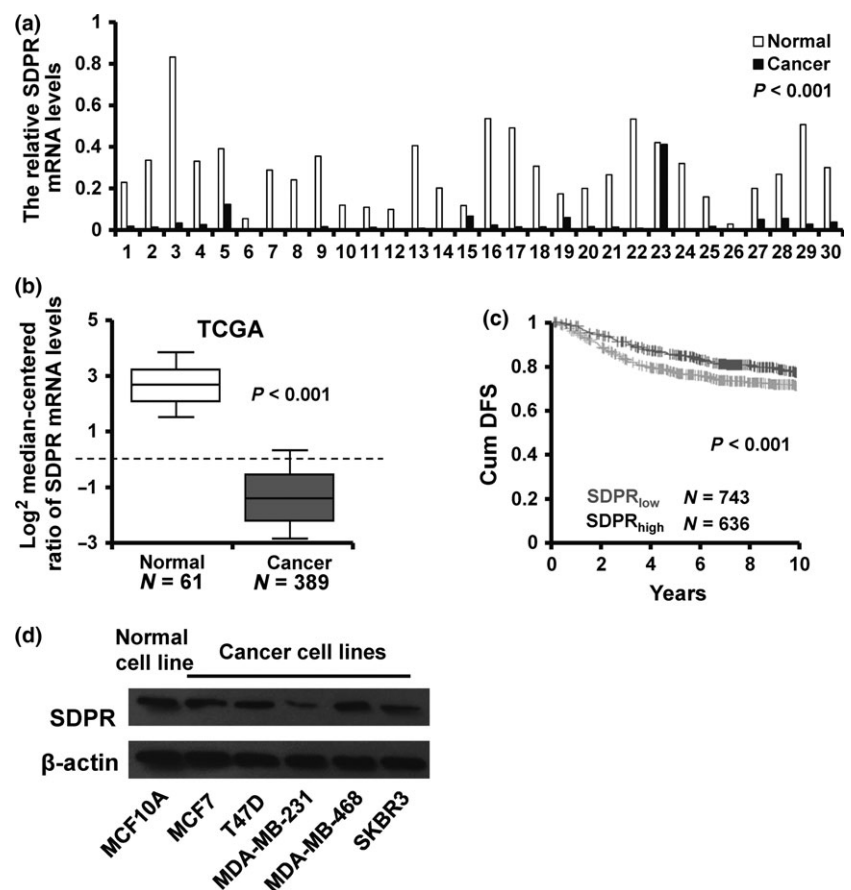


**Fig. 1.** Serum deprivation response (SDPR) is downregulated in breast cancer tissues. (a) RT-qPCR analysis of SDPR mRNA expression in breast cancer tissues and paired normal breast tissues. (b) Normalized SDPR mRNA levels analyzed based on gene expression profiling data from the Cancer Genome Atlas. (c) Kaplan-Meier analysis of breast cancer patients with different SDPR expression by GOBO. (d) Western blot analysis of SDPR protein expression in breast epithelial cell line MCF10A and indicated breast cancer cell lines.

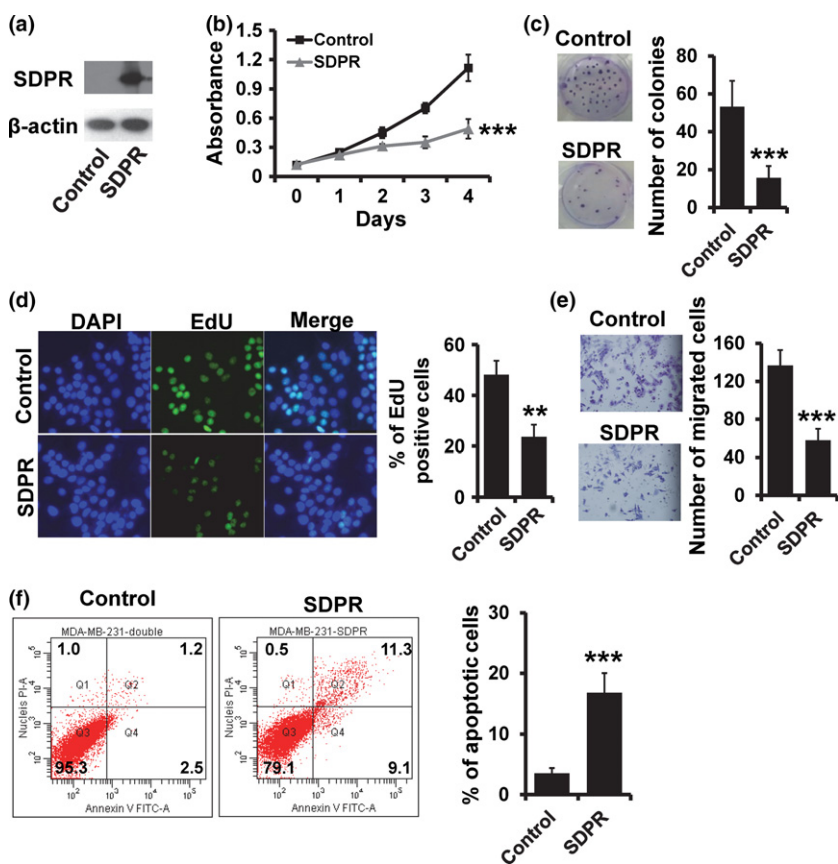


**Fig. 2.** Overexpression of serum deprivation response (SDPR) suppresses cell proliferation and invasion in MDA-MB-231 cell. (a) Western blot analysis of SDPR expression in 231-SDPR cells compared with vector control cells. (b–d) Cell proliferation analyzed by MTT (b), colony formation (c) and EdU (d) in 231-SDPR and vector control cells. (e) Transwell analysis of cell invasion in 231-SDPR and vector control cells. (f) The percentage of apoptotic cells in 231-SDPR and vector control cells. \*\**P* < 0.01, \*\*\**P* < 0.001.

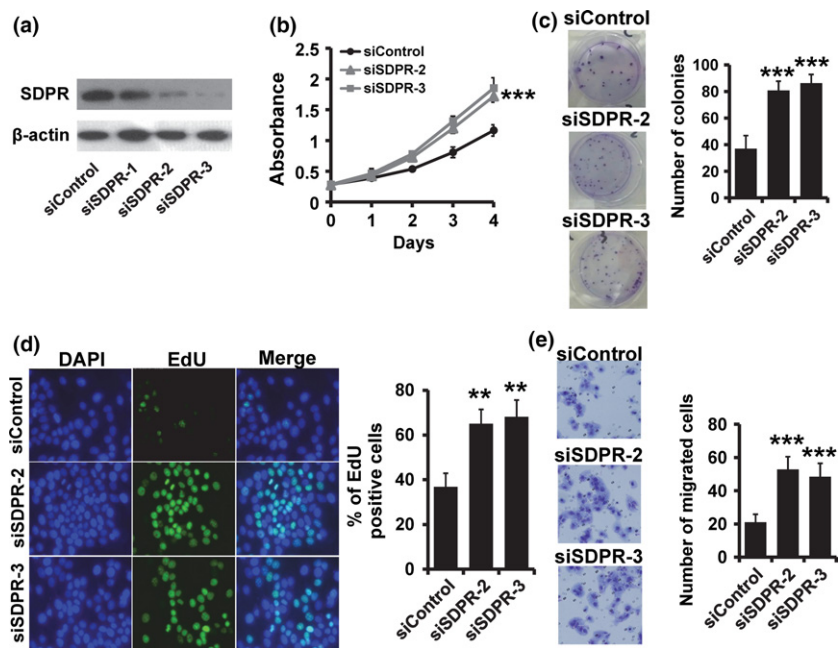


**Fig. 3.** Depletion of serum deprivation response (SDPR) stimulates cell proliferation and invasion in MCF10A cell. (a) Western blot analysis of SDPR expression in MCF10A-siSDPR cells compared with siControl cells. (b–d) Cell proliferation analyzed by MTT (b), colony formation (c) and EdU (d) in MCF10A-siSDPR and siControl cells. (e) Transwell analysis of cell invasion in MCF10A-siSDPR and siControl cells. \*\**P* < 0.01, \*\*\**P* < 0.001.

cells, the resultant PCR product of which was connected together with pcDNA3.1 tagged HA (SDPR-HA), and the resulting constructs were confirmed by DNA sequencing. For generation of stable cell lines expressing SDPR-HA, 2 days after transfection, MDA-MB-231 cells were transferred to a 10-cm cell culture dish and selected by medium with 1 mg/mL G418 for approximately 2 weeks. G418 resistant colonies were picked up and identified by western blot.

**Cell proliferation assay.** For MTT assay,  $5 \times 10^3$  cells were seeded in 96-well plates per well. Cell viability was examined over the next 5 days. After incubation, the cells were incubated with 20  $\mu$ L MTT (5 mg/mL in PBS; Sigma) at 37°C for 4 h. Then, the medium was removed and the formazan was dissolved in 150  $\mu$ L of DMSO (Sigma). The absorbance was measured at 570 nm using a micro-plate auto-reader (Bio-Rad).

For colony formation assay, 24 h after transfection, the cells were seeded into six-well plates at a density of 500 cells/well. After approximately 15 days, the cells grew to visible colonies and were stained with crystal violet. The colonies were counted and compared with control cells.

The EdU assay was detected by EdU labeling/detection kit (Ribobio) according to the manufacturer's protocol. Briefly, after transfection for 48 h, cells were incubated with 25  $\mu$ M EdU for 12 h. The cells were fixed with 4% formaldehyde for 30 min at room temperature and treated with 0.5% Triton X-100 for 15 min at room temperature for permeabilization. After being washed with PBS, cells were reacted with Apollo reaction cocktail for 30 min before fixation, permeabilization and EdU staining. Subsequently, cell nuclei were stained with Hoechst 33342 at a concentration of 5  $\mu$ g/mL for 30 min. The cells were then observed under a fluorescence microscope. The percentage of EdU-positive cells was examined by fluorescence microscopy.

**Invasion assay.** The invasion ability of breast cancer cells *in vitro* was evaluated by Matrigel coated Transwell inserts (BD Biosciences, San Diego, CA, USA).  $1 \times 10^5$  cells in 200  $\mu$ L FBS-free medium were added in the upper chamber of Transwell and 10% FBS-containing medium was added in the lower chamber. After 16 h, the cells were fixed by 4% paraformaldehyde and stained by Giemsa stain (Solarbio, Beijing, China). The cells were then observed under a microscope and the number of migrating cells was counted in five predetermined fields.

**Western blot.** Cells were lysed in RIPA buffer (containing 50 mM Tris-HCl, pH 7.4, 150 mM NaCl, 1% NP-40, 1 mM EDTA, 0.25% sodium deoxycholate), 1 mM NaF, 10 mM  $\text{Na}_3\text{VO}_4$ , 1 mM PMSF and protease inhibitor cocktail (Roche, Indianapolis, IN, USA). After incubation at 4°C for 30 min, the lysate was centrifuged at 15 000  $g$  for 10 min at 4°C. Protein concentration was determined using a BCA assay (Pierce, Rockford, IL, USA). Samples were denatured for 5 min at 95°C and subjected to 10% SDS/PAGE. The separated proteins were transferred to a PVDF membrane (Millipore, Bedford, MA, USA). The membrane was blocked in 5% (w/v) skim milk-TBST (10 mM Tris, 150 mM NaCl, 0.05% Tween 20, pH 8.3) solution, followed by incubation with the primary antibodies diluted in skim milk-TBST solution overnight at 4°C. The membrane was then incubated with the corresponding horseradish peroxidase-conjugated secondary antibody (Cell Signaling) for 1 h at room temperature, and immunoreactive protein bands were visualized by enhanced chemiluminescence reagents (Millipore).

**Immunofluorescence assay.** About  $5 \times 10^4$  cells were seeded in a 24-well plate. Cells were washed and fixed in 4% formaldehyde for 15 min at room temperature. The cells were then permeabilized with 1% Triton X-100 for 15 min at room temperature and blocked with 2% BSA for 30 min at room temperature. Cells were then incubated with primary antibody at 4°C overnight, followed by incubation with FITC-/TRITC-conjugated secondary antibodies for 1 h at room temperature, and then stained with DAPI. Finally, coverslips were observed under a fluorescence microscope.

**Flow cytometry analysis.** For cell cycle distribution assay, cells were fixed with 70% ethanol at  $-20^\circ\text{C}$  overnight and washed with PBS. Then, the cells were resuspended in 0.1% Triton-X100/PBS and concomitantly treated with Rnase A and stained with 50  $\mu$ g/mL propidium iodide (PI) for 15 min. The cell apoptosis assay was assessed by Annexin V Staining Kit (BD Biosciences). Cells were washed twice with PBS and resuspended in the binding buffer, before incubation with Annexin V and PI for 15 min at room temperature. The cell cycle distribution and apoptosis were analyzed using BD FACSCanto II.

**TGF $\beta$ 1 measurement with ELISA and TGF $\beta$  signaling assay.** Culture supernatants were harvested from treated breast cancer cells, centrifuged to remove cellular debris, and stored at  $-80^\circ\text{C}$ . TGF $\beta$ 1 protein levels were measured with a Human TGF $\beta$ 1 ELISA Kit (Abcam) according to the manufacturer's instructions. Each ELISA was carried out in duplicate for at least three separate experiments. TGF $\beta$  signaling activity was determined using Cignal SMAD Reporter Assay Kits (Qiagen, Hilden, Germany) according to the manufacturer's instructions. The SMAD reporter is a mixture of an inducible SMAD-responsive luciferase construct and a constitutively expressing Renilla construct.

**Statistical analysis.** All the experiments were performed at least twice independently and data presented as mean  $\pm$  SEM. All statistical analyses were performed using the SPSS 18.0 software system for Windows (SPSS). The statistical signifi-

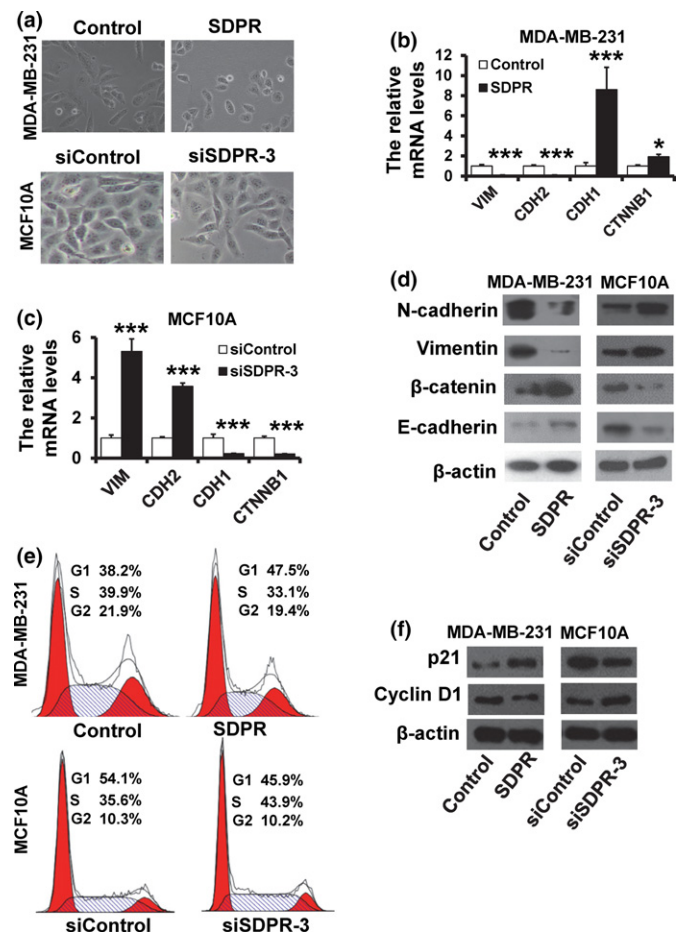


**Fig. 4.** Serum deprivation response (SDPR) depletion is linked to the epithelial-mesenchymal transition (EMT)-like phenotype. (a) Cellular morphology of the SDPR-overexpressed MDA-MB-231 (upper), SDPR-depleted MCF10A (lower), or appropriate control cells. (b-d) RT-qPCR analysis of mRNA expression of the mesenchymal markers Vimentin and N-cadherin (CDH2), and epithelial markers E-cadherin (CDH1) and  $\beta$ -catenin (CTNNB1) in the SDPR-overexpressed MDA-MB-231 (a), SDPR-depleted MCF10A (b) or appropriate control cells. (d) Western blot analysis of protein expression of the mesenchymal markers Vimentin and N-cadherin, and epithelial markers E-cadherin and  $\beta$ -catenin in the SDPR-overexpressed MDA-MB-231 (left) SDPR-depleted MCF10A (right), or appropriate control cells. (e) The cell cycle distribution of SDPR-overexpressed MDA-MB-231 (upper) SDPR-depleted MCF10A (lower), or appropriate control cells was analyzed by flow cytometry analysis. (f) Western blot analysis of protein expression of the Cyclin D1 and p21 in cells treated in (e). \* $P < 0.05$ , \*\*\* $P < 0.001$ .

cance of difference was calculated using Student's *t*-test, with significant differences defined as at least a *P*-value of <0.05.

## Results

**Serum deprivation response is downregulated in breast cancer.** To explore the influence of SDPR on breast cancer progression, we first examined the SDPR mRNA expression in 30 cases of paired normal and breast cancer tissues by reverse transcription quantitative PCR (RT-qPCR). SDPR expression was downregulated in 29/30 collected breast cancer tissues as compared with paired adjacent normal breast tissues (Fig. 1a). To further validate the relationship between SDPR expression and breast cancer progression, we analyzed an SDPR mRNA expression profiling dataset from the Cancer Genome Atlas (TCGA), including 389 cases of breast cancer tissues and 61 cases of normal breast tissues. The validation data confirmed that SDPR mRNA expression was downregulated in breast cancer tissues (Fig. 1b). Moreover, we compared the cumulative disease-free survival (DFS) between patients with high SDPR expression and low SDPR expression and found that the cumulative DFS with high SDPR expression is higher (red,

*N* = 636) than that of patients with low SDPR expression (gray, *N* = 743) by using GOBO (Fig. 1c). Next, we assessed the SDPR expression levels in various breast cancer cell lines and normal breast cell line by western blot. The result showed that the SDPR expression was downregulated in all breast cancer cell lines as compared to MCF10A cells (Fig. 1d). Taken together, these results indicated that SDPR is downregulated in breast cancer.

**Serum deprivation response is a tumor suppressor in breast cancer.** Next, we investigated the influence of SDPR on breast cancer cell proliferation and invasion by generation of stable SDPR-overexpressed MDA-MB-231 cell line (Fig. 2a). Overexpression of SDPR resulted in a lower proliferation rate in MDA-MB-231 cells as assessed by MTT (Fig. 2b), colony formation (Fig. 2c) and EdU (Fig. 2d) assays. Moreover, SDPR overexpression reduced cell invasion in MDA-MB-231 cells (Fig. 2e). We also observed that the apoptotic cells were significantly higher in SDPR-overexpressed MDA-MB-231 cells (Fig. 2f).

We then examined the effect of SDPR deficiency on the breast cancer cell proliferation and invasion. We used three specific siRNA targeting SDPR, and two of them could efficiently reduce the SDPR expression in MCF10A cells

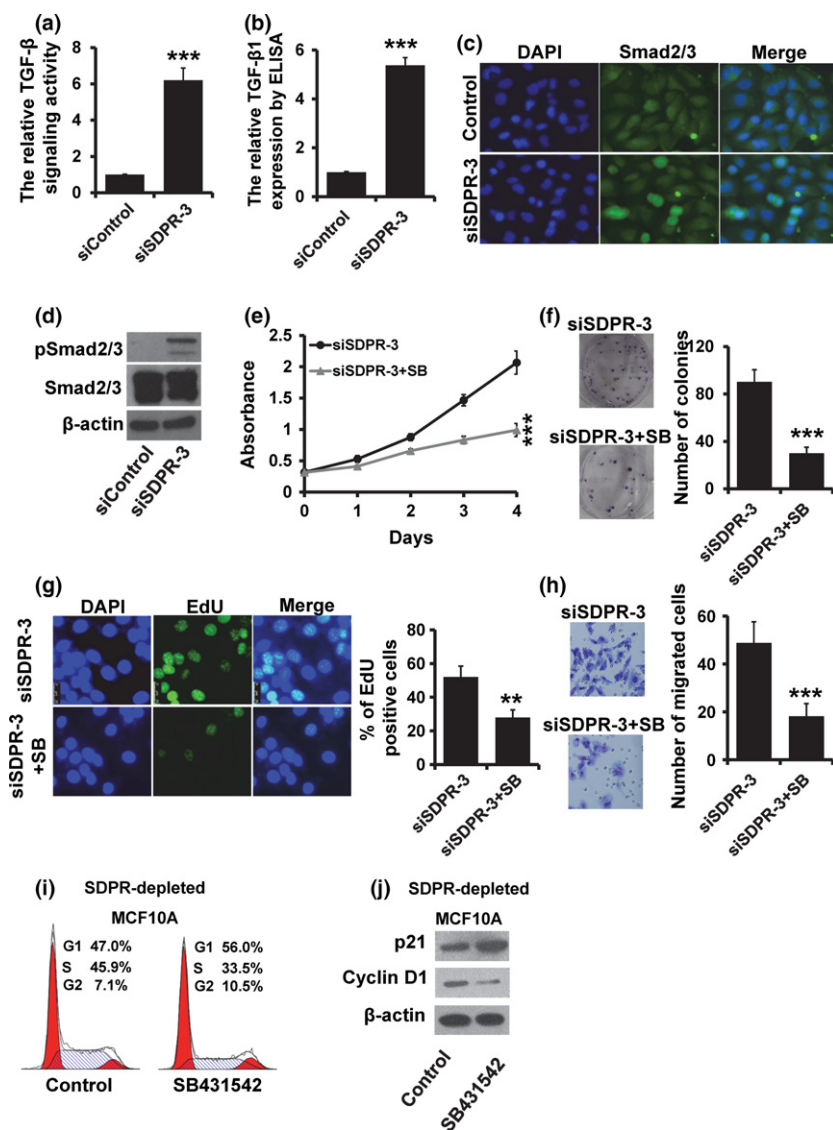


**Fig. 5.** Serum deprivation response (SDPR) depletion activates TGF-β signaling. (a) Luciferase reporter analysis of TGF-β signaling activity in MCF10A-siSDPR and siControl cells. (b) ELISA analysis of TGF-β1 expression in MCF10A-siSDPR and siControl cells. (c) Localization of Smad2/3 in MCF10A-siSDPR and siControl cells by immunofluorescence assay. (d) Western blot analysis of phospho-Smad2/3 expression in MCF10A-siSDPR and siControl cells. (e) Cell proliferation analyzed by MTT (e), colony formation (f) and EdU (g) in MCF10A-siSDPR with or without SB-431542 treatment. (h) Transwell analysis of cell invasion in MCF10A-siSDPR with or without SB-431542 treatment. (i) The cell cycle distribution of SDPR-depleted MCF10A cells with or without SB-431542 treatment was analyzed by flow cytometry analysis. (j) Western blot analysis of protein expression of the Cyclin D1 and p21 in cells treated in (i). \*\**P* < 0.01, \*\*\**P* < 0.001.

(Fig. 3a). By MTT assay, we found that depletion of SDPR resulted in a substantial increase in the rate of cell proliferation (Fig. 3b). The colony formation assay also showed that depletion of SDPR increased the number of colonies in MCF10A cells (Fig. 3c). Furthermore, the EdU assay confirmed that depletion of SDPR could promote breast cancer cell proliferation (Fig. 3d). The transwell assay showed that depletion of SDPR could promote breast cancer cell invasion (Fig. 3e).

Taken together, these results indicated that depletion of SDPR promotes breast cancer development and progression.

**Serum deprivation response suppresses epithelial–mesenchymal transition and blocks cells at G1 phase in breast cancer cells.** Epithelial–mesenchymal transition enables epithelial cells to acquire an invasive mesenchymal phenotype and is a critical mechanism for the initial step of metastasis.<sup>(12)</sup> We observed that MDA-MB-231 cells transfected with vector control retained their fibroblast-like morphology, whereas SDPR-overexpressed cells displayed a cobblestone-like morphology (Fig. 4a; upper). Compared with the siControl cells, SDPR depletion transformed MCF10A cells from a typical epithelial morphology into fibroblast-like shape (Fig. 4a; lower). To examine the effect of SDPR expression in breast cancer EMT, we measured the expression of epithelial and mesenchymal markers by RT-qPCR and western blot. SDPR-overexpressed MDA-MB-231 cells exhibited a significant downregulation of vimentin and N-cadherin (CDH2), while the epithelial markers E-cadherin (CDH1) and  $\beta$ -catenin (CTNNB1) were dramatically decreased by RT-qPCR (Fig. 4b) and western blot (Fig. 4d; left). In contrast, the vimentin and CDH2 was upregulated, while the CDH1 and CTNNB1 was downregulated in SDPR-depleted MCF10A cells by RT-qPCR (Fig. 4c) and western blot (Fig. 4d; right). These results showed that SDPR inhibits EMT-like phenotype in breast cancer cells.

Next, we analyzed the effect of SDPR expression on the cell cycle distribution by flow cytometry analysis. The percentage of cells at G1 phase was increased in SDPR-overexpressed MDA-MB-231 cells (Fig. 4e; upper), whereas the percentage of cells at S phase was increased in SDPR-depleted MCF10A cells (Fig. 4e; lower) compared with those of control cells. Furthermore, SDPR-overexpressed MDA-MB-231 exhibited an upregulation of the cell cycle inhibitor p21 and a downregulation of Cyclin D1. In contrast, p21 was downregulated, while Cyclin D1 was upregulated in SDPR-depleted MCF10A cells (Fig. 4f). These results indicated that SDPR blocks cells at G1 phase in breast cancer cells.

**Depletion of Serum deprivation response induces TGF- $\beta$  signaling.** Transforming growth factor- $\beta$  (TGF- $\beta$ ) is a pleiotropic cytokine which contributes to wound healing, angiogenesis, fibrosis and cancer.<sup>(12)</sup> We observed that the ability of cell proliferation and invasion was reduced after treatment with TGF- $\beta$  inhibitor SB431542 (Fig. S1a–d). Furthermore, SB431542 could inhibit the EMT-like phenotype in MDA-MB-231 cells (Fig. S1e). To investigate whether TGF- $\beta$  plays an important role in the function of SDPR, we performed a luciferase assay to determine the effect of SDPR on the TGF- $\beta$  signaling activity. As shown in Figure 5(a), the luciferase activity was significantly increased in SDPR-depleted MCF10A cells (Fig. 5a). The TGF- $\beta$ 1 expression was also elevated in SDPR-depleted MCF10A cells by ELISA assay (Fig. 5b). The immunofluorescence staining analysis showed that Smad2/3 translocated into the nucleus in SDPR-depleted MCF10A cells more than in the control cells (Fig. 5c). Furthermore, the expression of phosphorylated Smad2/3 were greatly increased in SDPR-depleted cells by western blot (Fig. 5d). The number of proliferating

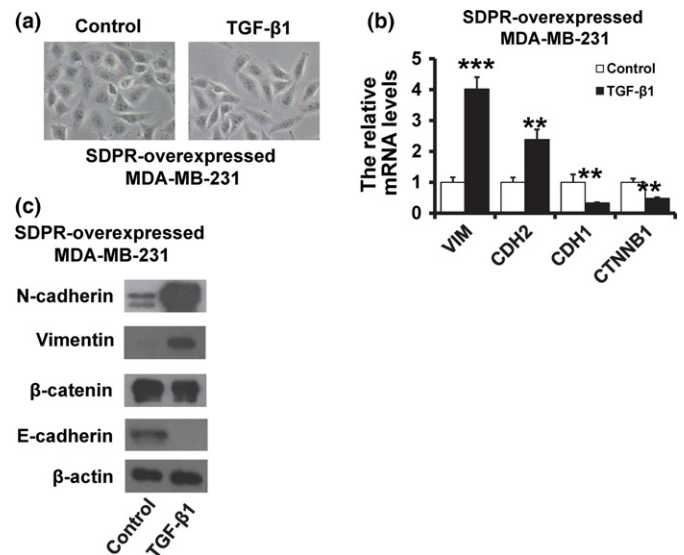


**Fig. 6.** Transforming growth factor- $\beta$  (TGF- $\beta$ ) restores the serum deprivation response (SDPR)-induced MET phenotype. (a) Cellular morphology of the SDPR-overexpressed MDA-MB-231 with or without TGF- $\beta$ 1 treatment. (b) RT-qPCR analysis of mRNA expression of the mesenchymal markers Vimentin and N-cadherin (CDH2), and epithelial markers E-cadherin (CDH1) and  $\beta$ -catenin (CTNNB1) in the SDPR-overexpressed MDA-MB-231 with or without TGF- $\beta$ 1 treatment. (c) Western blot analysis of protein expression of the mesenchymal markers Vimentin and N-cadherin, and epithelial markers E-cadherin and  $\beta$ -catenin in the SDPR-overexpressed MDA-MB-231 with or without TGF- $\beta$ 1 treatment.

cells was much lower in SDPR-depleted cells after treatment with TGF- $\beta$  inhibitor SB-431542 (Fig. 5e). Furthermore, the malignant phenotype induced by SDPR depletion was reversed by treatment with TGF- $\beta$  inhibitor SB-431542 (Fig. 5f–h). We also observed that the percentage of cells at S phase was dramatically decreased in SDPR-depleted MCF10A cells after treatment with SB431542 (Fig. 6i). Furthermore, the expression of p21 was elevated, while the expression of Cyclin D1 was decreased after treatment with SB431542 (Fig. 6j).

To further confirm that SDPR mediated breast cancer progression through regulating TGF- $\beta$  signaling, we added TGF- $\beta$ 1 in SDPR-overexpressed MDA-MB-231 cells. We observed that addition of TGF- $\beta$ 1 restored the fibroblast-like morphology (Fig. 6a). Moreover, the expression of epithelial markers was downregulated, while the mesenchymal markers were elevated after treatment with TGF- $\beta$ 1 by RT-qPCR (Fig. 6b) and western blot (Fig. 6c). Together, these results suggested that downregulation of SDPR promotes breast cancer progression through activation of TGF- $\beta$  signaling.

## Discussion

In the present study, we determined the role of SDPR in breast cancer progression. We observed that SDPR expression was downregulated in breast cancer tissues. Overexpression of SDPR suppressed breast cancer progression, while depletion of SDPR promoted breast cancer progression. Furthermore, the results showed that SDPR depletion induced EMT and activated TGF- $\beta$  signaling.

Several reports have suggested that SDPR is most frequently downregulated in cancer tissues, including in breast, kidney and prostate cancer.<sup>(8–10)</sup> Consistent with these studies, our findings demonstrated that SDPR is poorly expressed in breast

cancer tissues. Sharan *et al.* (2015) indicated that SDPR suppresses cell proliferation and migration in 293FT cells.<sup>(11)</sup> Thus, we further assessed whether SDPR suppresses the proliferation and invasion in breast cancer cells. We found that ectopic expression of SDPR could reduce cell proliferation and invasion, and promote cell apoptosis in MDA-MB-231 cells. Moreover, depletion of SDPR enhanced the cell proliferation and invasion in MCF10A cells. Together, these results demonstrated that SDPR suppresses cell proliferation and invasion in breast cancer cells. Based on the gene expression profiling, a molecular classification has been proposed to classify breast cancer into five different subtypes: Luminal A, Luminal B, Basal, HER2+ and normal-like.<sup>(13)</sup> Based on these subtypes, breast cancer patients can be divided into groups with distinct tumor morphologies, prognosis and responses to therapies.<sup>(14)</sup> The role of SDPR in breast cancer differentiation needs to be clarified in future.

Epithelial–mesenchymal transition is a key process underlying tumor cell dissemination from the primary tumor to distant organs. During EMT, epithelial cells lose their cell polarity and molecular expression, enabling cell–cell adhesion, and they gain migratory and invasive properties.<sup>(15,16)</sup> Lack of SDPR contributes not only to the morphology of the basal plasma membrane, but also to the maintenance of epithelial polarity during early pregnancy.<sup>(17)</sup> In our study, we found that SDPR decreases

EMT programs in human breast cancer cells, including upregulation of epithelial markers (E-cadherin and  $\beta$ -catenin) and downregulation of mesenchymal markers (Vimentin and N-cadherin). These findings demonstrated that SDPR inhibits EMT phenotype in breast cancer cells. TGF- $\beta$  is a multi-functional regulator of cell growth, apoptosis, differentiation and migration.<sup>(18)</sup> Many studies suggest that transforming growth factor- $\beta$  (TGF- $\beta$ ) can induce EMT.<sup>(12,19,20)</sup> TGF- $\beta$  signaling pathway has been considered as an activator of cancer progression. We observed that depletion of SDPR could elevate the expression of TGF- $\beta$ 1 and activate TGF- $\beta$  signaling.

In conclusion, we demonstrated that SDPR is downregulated in breast cancer tissues and SDPR suppresses breast cancer progression by blocking TGF- $\beta$ -induced EMT.

### Acknowledgments

This study was supported by the National Natural Science Foundation of China (Nos 81372843, 81472472 and 81502518), and the National Science and Technology Support Program (No. 2015BAI12B15).

### Disclosure Statement

The authors have no conflict of interest to declare.

### References

- Cheang MC, Voduc D, Bajdik C *et al.* Basal-like breast cancer defined by five biomarkers has superior prognostic value than triple-negative phenotype. *Clin Cancer Res* 2008; **14**: 1368–76.
- Siegel R, Naishadham D, Jemal A. Cancer statistics, 2015. *CA Cancer J Clin* 2015; **65**: 5–29.
- Gustincich S, Vatta P, Goruppi S *et al.* The human serum deprivation response gene (SDPR) maps to 2q32–q33 and codes for a phosphatidylserine-binding protein. *Genomics* 1999; **57**: 120–9.
- Baig A, Bao X, Wolf M, Haslam RJ. The platelet protein kinase C substrate pleckstrin binds directly to SDPR protein. *Platelets* 2009; **20**: 446–57.
- Hansen CG, Bright NA, Howard G, Nichols BJ. SDPR induces membrane curvature and functions in the formation of caveolae. *Nat Cell Biol* 2009; **11**: 807–14.
- Gupta R, Toufaily C, Annabi B. Caveolin and cavin family members: dual roles in cancer. *Biochimie* 2014; **107**: 188–202.
- Drab M, Verkade P, Elger M *et al.* Loss of caveolae, vascular dysfunction, and pulmonary defects in caveolin-1 gene-disrupted mice. *Science* 2001; **293**: 2449–52.
- Li X, Jia Z, Shen Y *et al.* Coordinate suppression of Sdpr and Fhl1 expression in tumors of the breast, kidney, and prostate. *Cancer Sci* 2008; **99**: 1326–33.
- Gianazza E, Chinello C, Mainini V *et al.* Alterations of the serum peptidome in renal cell carcinoma discriminating benign and malignant kidney tumors. *J Proteomics* 2012; **76**: 125–40.
- Bai L, Deng X, Li Q *et al.* Down-regulation of the cavin family proteins in breast cancer. *J Cell Biochem* 2012; **113**: 322–8.
- Sharan A, Zhu H, Xie H *et al.* Down-regulation of miR-206 is associated with Hirschsprung disease and suppresses cell migration and proliferation in cell models. *Sci Rep* 2015; **5**: 9302.
- Yu Y, Xiao CH, Tan LD, Wang QS, Li XQ, Feng YM. Cancer associated fibroblasts induce epithelial–mesenchymal transition of breast cancer cells through paracrine TGF- $\beta$  signalling. *Br J Cancer* 2014; **110**: 724–32.
- Neve RM, Chin K, Fridlyand J *et al.* A collection of breast cancer cell lines for the study of functionally distinct cancer subtypes. *Cancer Cell* 2006; **10**: 515–27.
- Du X, Li XQ, Li L, Xu YY, Feng YM. The detection of ESR1/PGR/ERBB2 mRNA levels by RT-QPCR: a better approach for subtyping breast cancer and predicting prognosis. *Breast Cancer Res Treat* 2013; **138**: 59–67.
- Bill R, Christofori G. The relevance of EMT in breast cancer metastasis: correlation or causality? *FEBS Lett* 2015; **589**: 1577–87.
- Bedi U, Mishra VK, Wasilewski D, Scheel C, Johnsen SA. Epigenetic plasticity: a central regulator of epithelial-to-mesenchymal transition in cancer. *Oncotarget* 2014; **5**: 2016–29.
- Madawala RJ, Poon CE, Dowland SN, Murphy CR. PTRF is associated with caveolin 1 at the time of receptivity: but SDPR is absent at the same time. *Histochem Cell Biol* 2015; **143**: 637–44.
- Liu Y, Hu H, Wang K *et al.* Multidimensional analysis of gene expression reveals TGF $\beta$ 111-induced EMT contributes to malignant progression of astrocytomas. *Oncotarget* 2014; **5**: 12593–606.
- Horiguchi K, Sakamoto K, Koinuma D *et al.* TGF- $\beta$  drives epithelial–mesenchymal transition through  $\delta$ E1-mediated downregulation of ESRP. *Oncogene* 2012; **31**: 3190–201.
- Saitoh M. Epithelial–mesenchymal transition is regulated at post-transcriptional levels by transforming growth factor- $\beta$  signaling during tumor progression. *Cancer Sci* 2015; **106**: 481–8.

### Supporting Information

Additional supporting information may be found in the online version of this article:

**Fig. S1.** TGF- $\beta$  inhibitor SB431542 suppresses cell proliferation and invasion in MDA-MB-231.

**Data S1.** Supplementary material.